Analysis of Heavy Metal Toxic Ions by Adsorption onto Amino-functionalized Ordered Mesoporous Silica†

Ali Md Showkat,[‡] Yu-Ping Zhang,[§] Min Seok Kim,[‡] Anantha Iyengar Gopalan,[‡,#] Kakarla Raghava Reddy,[‡] and Kwang-Pill Lee[‡,#,*]

[‡]*Department of Chemistry Graduate School, Kyungpook National University, Daegu 702-701, Korea.* [*]*E-mail: kplee@knu.ac.kr*
[§]*Henan Institute of Science and Technology, Xinxing 453003, P.R. China*
[#]*Nano Practical Application Center, Daegu 704-801, Korea*
Received June 6, 2007

Ordered mesoporous silica (MCM-41) materials with different textural properties were prepared using alkyl (dodecyl, cetyl, eicosane) trimethyl ammonium bromide (DTAB, CTAB, ETAB, respectively) as structure directing surfactants, functionalized with amine groups and used as adsorbent for the toxic metal ions, Cr (VI), As (V), Pb (II) and Hg (II). Amino functionalization of mesoporous MCM-41 was achieved by co-condensation of N-[3-(trimethoxysilyl)-propyl] aniline with tetraethyl orthosilicate. Adsorption isotherm and adsorption capacity of the amine functionalized materials for Cr (VI), As (V), Pb (II) and Hg (II) ions were followed by inductively coupled plasma mass spectrometry (ICP-MS). Results demonstrate that amine functionalized MCM-41 prepared with ETAB showed higher adsorption capacity for Cr (VI), As (V), Pb (II) and Hg (II) ions in comparison to MCM-41 prepared with CTAB and DTAB. The higher adsorption capacity for MCM-41(ETAB) was correlated with amine content in the material (determined by CHN analysis) and relative decrease in pore volume and pore diameter. X-ray diffraction (XRD) analysis, nitrogen adsorption-desorption measurements and Fourier Transform infrared spectrometry (FTIR) were used to follow the changes in the textural parameters and surface properties of the mesoporous materials as a result of amine functionalization to correlate with the adsorption characteristics. The adsorption process was found to depend on the pH of the medium.

Key Words : Mesoporous, Textural parameters, Adsorbent, Heavy metal ions, MCM-41

Introduction

Mesoporous silica materials[1,2] have attracted attention because of their utilities in adsorption, selective separation and catalysis.[3-6] MCM-41, one of the important mesoporous materials, has excellent periodicities in the mesoporous channels, larger BET surface area, high porosities and narrow pore sizes.[7-9] Initial studies of the self-assembled silicas having a two-dimensional hexagonal ordering of cylindrical mesopores stimulated activities on the preparation of several mesoporous materials using alkyltrimethylammonium surfactants of varying alkyl chain length as structure directing agents. Interestingly, the textural parameters of MCM-41 can be tuned by selecting the suitable structure directing agent and experimental conditions. And, this strategy can be successfully utilized for synthesizing highly ordered MCM-41 materials with pore diameters ranging from 3.0 nm to 6.5 nm by using alkyltrimethylammonium surfactants with alkyl chains having 10 to 22 carbon atoms.[10,11] Recently, we have prepared a few mesoporous materials of tunable textural parameters and used to nanostructure conducting polymers inside the channels of the materials.[12,13]

Functionalized mesoporous materials have shown to exhibit a few remarkable properties that suit for applications in catalysis, adsorption, and environmental remediation.[14,15] Metal ion adsorbents have been prepared by grafting thiol functional groups as a monolayer onto the inner surface of MCM-41.[16,17] Thiol functionalized MCM-41 was proved to be efficient adsorbents for mercury and heavy metal ions. A few other reports are available on synthesis thiol and amine functionalized mesoporous materials and use of the functionalized MCM-41 as adsorbents for removal of heavy metal ions.[18-20] Brunel *et al.*[21] have incorporated amino groups in the mesopores through reaction of 3-halopropyl-silated mesoporous materials with amines.

The removal of polluting oxyanions, like arsenate[22-24] and chromate[25,26] ions from water has attracted a great deal of interest. Removal of Cr ions needs considerable attention as several industries of areas like textile, leather, tanning, electroplating, pigmentation and dyes are expelling the chromium ions into the environment at concentrations higher than the threshold limits to cause pollution.[27] Unlike the other heavy metals, Cr and As ions occur as tetrahedral oxyanions (arsenate and chromate) in the hydrosphere.[28] Also, metal ions such as Pb (II) and Hg (II) are known to cause pollution of water and ecosystems. Several methods such as co-precipitation,[29,30] reverse osmometry,[31] and adsorbing colloid flotation methods[32] have been employed for the removal toxic oxyanions. However, these methods require adequate infrastructure in the form of equipments

† This paper is dedicated to Professor Sang Chul Shim on the occasion of his honorable retirement.

and reagents. Mechanisms of arsenate ion adsorption by highly-ordered nano-structured silicate media impregnated with metal oxides were studied.[33] Loading of metal oxides into highly ordered mesoporous silica, SBA-15 was achieved by incipient-wetness impregnation technique and the loaded silicas were used to follow the arsenate adsorption behavior. Uptake of arsenate, chromate, selenate, and molybdate at the Fe (III) ions adsorption sites present in channels of MCM-41 was followed.[34] Adsorption has been utilized for the removal of pollutant metal cations using activated carbon,[35,36] polymers,[37] zeolites,[38,39] and clays.[40,41] The adsorption of pollutant metal cations by functionalized mesoporous silicas containing amino or thiol groups has been previously investigated.[42-44]

In the present work, we have prepared a few mesoporous materials using surfactants having different lengths of aliphatic chains as the structure directing agents. Dodecyltrimethyl ammonium bromide (DTAB), cetyltrimethyl ammonium bromide (CTAB) and eicosanetrimethyl ammonium bromide (ETAB) were used as surfactants. MCM-41 materials were independently synthesized using DTAB, CTAB and ETAB. MCM-41 materials were amine functionalized by co-condensation with N-[3-(trimethoxysilyl)-propyl] aniline (Scheme1) to obtain N-MCM-41-D; N-MCM-41-C and N-MCM-41-E, where N stands for amine functionalization, and D, C and E stand for DTAB, CTAB and ETAB. As anticipated, there were significant differences in the textural and structural parameters among N-MCM-41-D, N-MCM-41-C and N-MCM-41-E as evident from X-ray diffraction, nitrogen adsorption - desorption measurements and FTIR spectrometry. The amine-functionalized MCM-41 materials with varying textural parameters were used as model adsorbents to study the adsorption of toxic metal ions, $HAsO_4^{2-}$, As(V)CrO_4^{2-}, Cr(VI), Pb(II) and Hg(II) ions. The adsorption capacities of amine-functionalized MCM-41 materials are discussed in terms of textural properties.

Experimental Section

Tetraethyl orthosilicate (TEOS), cetyl trimethyl ammonium bromide (CTAB), 1-bromodecane, 1-bromoeicosane, N-[3-(trimethoxysilyl)-propyl]aniline and triethyl amine were purchased from Aldrich Chemicals Co. (Milwaukee, USA). Potassium chromate (K_2CrO_4 > 99%) and potassium arsenate (KH_2AsO_4) were obtained from Hayashi pure chemical industries Ltd, Korea [arsenate and chromate solutions are toxic and should be treated wearing impermeable gloves and goggles in order to avoid contact with skin and eyes]. Lead (II) nitrate ($Pb(NO_3)_2$) and mercury(II) nitrate ($Hg(NO_3)_2$) were obtained from Aldrich Chemicals Co. (Milwauke, USA). Other high purity chemicals were used as received.

Mesoporous materials (MCM-41) were prepared[45] by using DTAB, CTAB and ETAB as surfactants. DTAB and CTAB were synthesized. For the synthesis of DTAB, a solution of 1-bromodecane (7.5 mL) was mixed with triethyl amine (5.0 mL) in chloroform (30.0 mL). The mixture was refluxed at 80 °C and stirred for 24 h. A white powder (DTAB) was obtained after evaporation of chloroform and drying in a vacuum oven. ETAB was prepared through a similar method to DTAB, by the reaction of 1-bromoeicosane with triethylamine. Synthesis of MCM-41 was performed as described elsewhere.[12,13,46-49] DTAB, CTAB and ETAB were used as surfactants. A typical procedure[12] for the preparation of MCM-41 is given. CTAB/DTAB/ETAB was diluted with water and stirred for 10 min. Ammonia and ethanol were subsequently added under stirring to obtain a

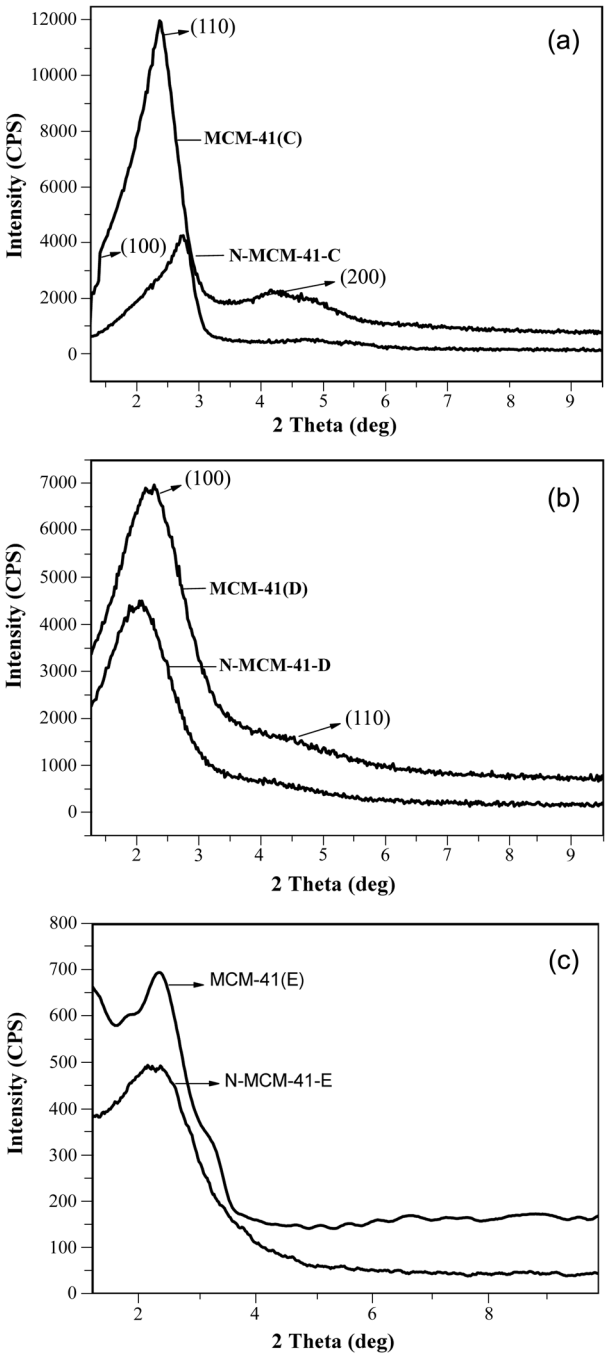

Figure 1. XRD patterns of pristine MCM-41(C) and N-MCM-41-C (a); pristine MCM-41(D) and N-MCM-41-D (b); pristine MCM-41(E) and N-MCM-41-E (c).

clear solution. An aqueous solution of TEOS was prepared. The solution of CTAB/DTAB/ETAB was added drop wise to the solution of TEOS. After stirring continuously for 4 h, a gel (molar) having the composition: 0.024 TEOS; 0.0024 surfactant (CTAB/DTAB/ETAB); 0.14 aqueous ammonia; 2.568 water; 1.284 ethanol was obtained. The gel was calcined in an oven at 550 °C. The calcined mass from the gel prepared with DTAB, CTAB and ETAB were designated as MCM-41(C) MCM-41(D) and MCM-41(E), respectively. 0.5 g of the MCM-41(C) or MCM-41 (D) and MCM-41 (E) was placed in 100 mL of toluene and stirred for 30 min, and 1 mL of N-[3-(trimethoxysilyl)-propyl] aniline was added to the resulting mixture. The mixture was stirred for 8 h at 60 °C. The solid mass was washed, filtered and dried under vacuum. The mass obtained from MCM-41(C), MCM-41(D) and MCM-41(E) was designated as N-MCM-41-C, N-MCM-41-D and N-MCM-41-E, where N stands for amine functionalization. Adsorption experiments were carried out with the oxyanions, KH_2AsO_4 or K_2CrO_4 and metal ions Pb (II) or Hg (II) individually as adsorbate. A typical adsorption experiment is outlined below. 50 mg of N-MCM-41-C or N-MCM-41-D or N-MCM-41-E was stirred at 25 °C in 10 mL of an aqueous solution containing of KH_2AsO_4 or K_2CrO_4 or $Pb(NO_3)_2$ or $Hg(NO_3)_2$. The adsorbent was removed by filtration after a specific time of adsorption.

The concentration of the residual metal ion (As (V), Cr (VI), Pb (II) and Hg (II)) in the solution was analyzed by inductively coupled plasma mass (ICP-MS) spectrometry. The amount of adsorbed metal ion was estimated from the difference between initial and final concentrations in the solution. Distribution coefficient, K_d of the oxyanion/metal ions was determined as the amount of oxyanion adsorbed per unit weight (g) of adsorbent with respect to concentration of oxyanion in 1 mL of the solution. The synthetic aqueous solutions (spike samples) were prepared by dissolving the relevant heavy metal salts in distilled water. Solutions of different pH were prepared by the addition of 1 M HNO_3 or NaOH to the aqueous solution containing the heavy metal ion. The adsorption behavior of the amine functionalized silica adsorbent toward the metal ions was followed at different pH values. N-MCM-41-C, N-MCM-41-D, N-MCM-41-E were characterized by X-ray diffraction (XRD) analysis and the XRD patterns were collected by employing a D_8-Advanced Bruker AXS diffractometer using CuKα1 radiation (λ = 1.54056A°) with (θ-2θ) geometry using a scintillation counter (low-angle region). Nitrogen adsorption-desorption (BET- Brunauer- Emmett- Teller) isotherms were collected using a quantachrome Autosorb-1 with nitrogen as adsorbate at 77 K. The samples were degassed for 12 h at 300 °C under vacuum before measurement.

Pore sizes were obtained from adsorption branches of isotherms using the Barret-Joynes-Halenda model for cylindrical pores. Elemental compositions (% of carbon, hydrogen and nitrogen) of N-MCM-41-C or N-MCM-41-D or N-MCM-41-E were determined by FISONS EA 1110 elemental analyzer equipped with a flash combustion furnace. FTIR spectra of the samples were recorded in mid IR (400-4000 cm^{-1}) region on a Jasco 610 spectrometer at 4 cm^{-1} resolution. Compressed KBr pellets containing 6% sample were used for this purpose. Each spectrum was collected after 100 co-added scans. Analysis of toxic ions was carried out by ICP-mass spectrometry (ICP-MS, Perkin Elmer Exlan 6000). Arsenic and chromium contents were determined. pH measurements were made using a pH meter model-250 (Thermo, orion, Beverly MA01915, USA).

Results and Discussion

We have checked the XRD patterns of the mesoporous materials, before and after the functionalization with N-[3-(trimethoxysilyl)-propyl] aniline. XRD patterns (Fig. 1) of MCM-41(D), MCM-41 (C) and MCM-41(E) are compared with N-MCM-41-D, N-MCM-41-C and N-MCM-41-E, respectively. XRD diffractions of pristine MCM-41(D), MCM-41(C) and MCM-41(E) showed an intense (100) reflection (major reflection) and one or a few additional weak peaks for higher order reflections. These reflection patterns are attributed to the 2D hexagonal structure (p6 mm) of mesoporous material.[2]

However, after amine functionalization (Scheme 1), the XRD patterns showed significant decrease in intensities with peak broadening for (100) reflections. The intensity decrease for higher order reflections resulted an apparent loss of XRD patterns for these reflections in N-MCM-41. Additionally, comparison of XRD patterns of MCM-41(C) and N-MCM-

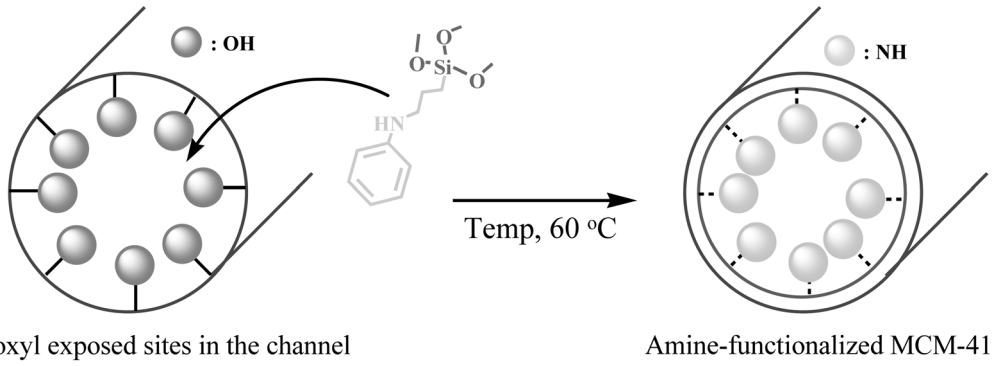

Scheme 1. Preparation of amine functionalized MCM-41 (N_MCM-41).

Table 1. BET surface area, total pore volume, pore size and loading of N of functionalized mesoporous silica

	S_{BET} ($m^2.g^{-1}$)	V_P ($mm^3.g^{-1}$)	2 R_{Pa} (nm)	Relative decrease (%)			N content ($mmol.g^{-1}$)
				ΔS_{BET}	ΔV_P	ΔR_{Pa}	
MCM-41(D)	1120	248	3.3				0
N-MCM-41-D	504	132	2.9	55.0	46.7	12.1	1.8
MCM-41(C)	1045	214	3.1				0
N-MCM-41-C	580	138	2.8	44.5	35.5	9.7	1.6
MCM-41(E)	1278	281	3.1				0
N-MCM-41-E	575	134	2.7	56.0	52.3	12.9	2.1

[a]After BJH pore size distributions.

41-C revealed that the dominant (100) reflection that appeared at 2.37° for MCM-41(C) was found to be shifted to 2.82° for N-MCM-41-C. Comparatively, MCM-41(C) changed into more disordered structure after functionalization in comparison with MCM-41(D) and MCM-41(E). The changes in XRD pattern between MCM-41 and N-MCM-41 are attributed to several factors. Higher contrast between silica and organic groups, loss of space correlations of the pores (as evident from the pore size changes-discussed in the latter part) and loss of meso structural order may be attributed as the reasons for the changes in XRD pattern. Similar types of disorder in silica mesostructure have been previously reported.[49-52]

Despite the absence of reflections of higher order indices, the major reflection (100) was retained in the amine functionalized silica materials. This implied that even after functionalization, the mesostructure ordering in MCM-41(C), MCM-41(D), and MCM-41(E) was retained. The results of nitrogen adsorption-desorption measurements (BET, surface area, pore volume and pore size through BJH distributions) were used to compare the textural parameters between pristine MCM-41(C), MCM-41(D), MCM-41(E) and N-MCM-41-D, N-MCM-41-C and N-MCM-41-E, respectively (Table 1). BET specific surface area, pore volume and pore size of amine functionalized MCM-41 are comparatively lower than those of the corresponding pristine materials, MCM-41(D), MCM-41(C) and MCM-41(E). For example, BET surface area of 1120 $m^2 \cdot g^{-1}$, pore volume of 248 $mm^3 \cdot g^{-1}$ and pore diameter of 3.3 nm that were noticed for pristine MCM-41 (D), subsequently decreased to 504 $m^2 \cdot g^{-1}$, 132 $mm^3 \cdot g^{-1}$ and 2.9 nm, respectively in N-MCM-41-D.

Similar trends were noticed with MCM-41(C) and MCM-41(E). Such a decrease in values of textural parameters is attributed to the formation of organic layer in the channels of MCM-41. Interestingly, the extent of decrease in these textural parameters was found to be different for MCM-41(D), MCM-41(C) and MCM-41(E). Relative decrease in the textural parameters, BET surface area (ΔS_{BET}), pore volume (ΔV_P) and pore radius (ΔR_P) upon functionalizing the MCM-41 with amine groups was calculated (Table 1) from the difference in the textural parameter between pristine and amine functionalized material to the value of the textural parameter of pristine MCM-41. A few interesting observations could be noticed on comparing the relative decrease in the values of textural parameters. MCM-41(C) showed a lower decrease in surface area, pore volume and pore diameter, in comparison to MCM-41(D) and MCM-41(E). And, MCM-41(E) showed higher values for ΔS_{BET}, ΔV_P and ΔR_{PA} in comparison to MCM-41(D) and MCM-41(C) (Table 1). ΔS_{BET}, ΔV_P and ΔR_{PA} for MCM-41(C) were 44.5%, 35.5% and 9.7%, respectively. For MCM-41(C) the values were 55.0%, 46.7% and 12.1%. Likewise, for MCM-41(E), ΔSBET, ΔVP and ΔRPA, values were 56.0%, 52.3% and 12.9%, respectively (Table 1).

Knowing the fact that there are changes in the relative decrease in textural parameter as a result of amine functionalization, the change in textural parameters was correlated with the extent of amine functionalization. Hence, nitrogen (N) content of the functionalized materials were determined and represented as mmol/g of the materials (Table 1). It can be seen from Table 1 that N content of MCM-41(E), MCM-41(C) and MCM-41(D) takes the following order: N-MCM-41-E > N-MCM-41-D > N-MCM-41-C. The larger decrease in pore volume (52.3%) and pore diameter (12.9%) for MCM-41(E) after amine functionalization is attributed to the higher extent of amine functionalization (2.1 $mmol \cdot g^{-1}$). MCM-41(C) showed the lowest extent of (1.6 $mmol \cdot g^{-1}$) amine functionalization among the selected MCM-41 materials and this is reflected in the lowest decrease in textural parameters for MCM-41(C) (Table 1).

FTIR spectra of MCM-41(D), MCM-41(C), MCM-41(E), N-MCM-41-C, N-MCM-41-D and N-MCM-41-E are presented (Fig. 2). The sharp band appearing around 3400 cm^{-1} in all the MCM-41 materials has been assigned to isolated Si-OH and the other bands were attributed to the contributions of hydrogen bonded silanols.[53] Besides, we could notice a few changes in the infra red bands of MCM-41 after functionalization with amine groups. Bands characteristics of NH_2 scissor bands were observed around 1100 cm^{-1} and 1630 cm^{-1} in N-MCM-41-C, N-MCM-41-D and N-MCM-41-E.[54]

The adsorption isotherms of As (V), Cr (VI), Pb (II) and Hg (II) metal ions were followed using N-MCM-41-D, N-MCM-41-C and N-MCM-41-E as adsorbents (Fig. 3). Different trends were noticed in the uptake of oxyanions by the N-MCM-41-D, N-MCM-41-C and N-MCM-41-E. The extent of uptake of metal ions, saturation level of adsorption and equilibrium concentration of the adsorbate to acheive the saturation limit for the amine functionalized silicas were

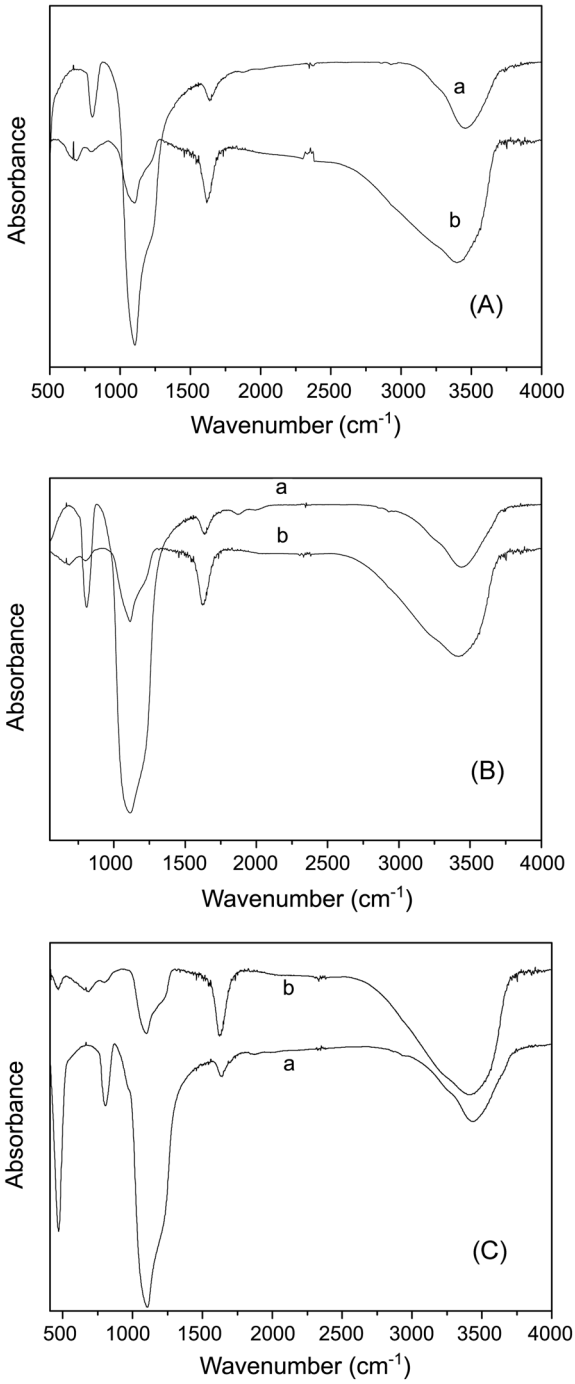

Figure 2. FTIR spectrum of pristine MCM-41(C) (a) and N-MCM-41-C(b)(A); pristine MCM-41(D) (a) and N-MCM-41-D (b)(B); pristine MCM-41(E) (a) and N-MCM-41-E (b)(C)

found to depend on the textural parameters. In general, the uptake of As (V), Cr (VI), Pb (II) and Hg (II) metal ions gradually increased with equilibrium concentration of oxyanions used for adsorption and finally reached a saturation limit with any of the amine functionalized silica adsorbent (Fig. 3).

A maximum adsorption (0.85 mmol.g^{-1}) was observed for As (V) oxyanions with an increased extend of uptake per unit equilibrium concentration of the adsorbate for N-MCM-41-E. This can be inferred from the higher initial slope in the adsorption isotherms for N-MCM-41-E in comparison to the N-MCM-41-C and N-MCM-41-D. Hence, it was inferred that N-MCM-41-E has the highest capacity for As (V) adsorption among the three amine functionalized mesoporous materials used in this study. The higher extent of As (V) oxyanion uptake for N-MCM-41-E correlates with higher N content for N-MCM-41-E in comparison to N-MCM-41-D and N-MCM-41-C (Table 2).

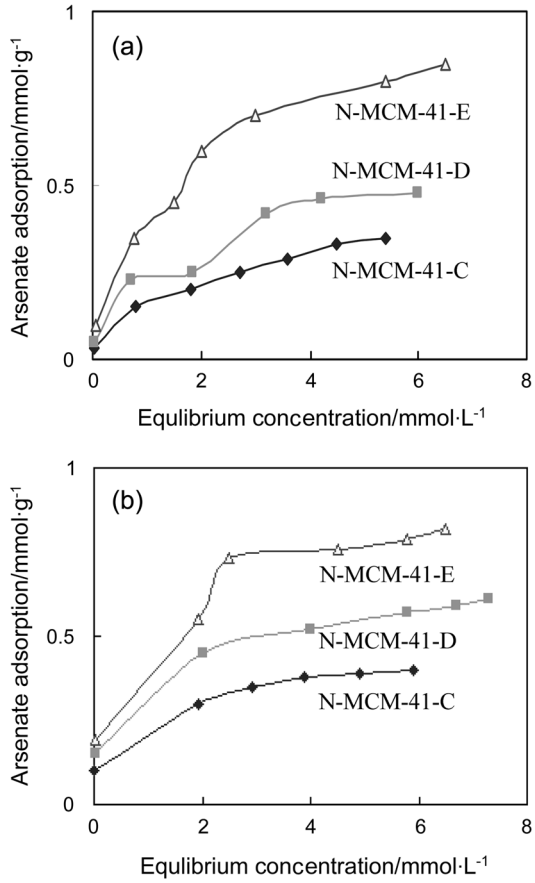

Figure 3. Adsorption isotherms of (a) arsenate and (b) chromate oxyanions on functionalized MCM-41.

The adsorption capacity of MCM-41(E) towards As (V) anions was 1.8 times higher than N-MCM-41-D and 3.1 times higher than N-MCM-41-C. The lower relative decrease in pore volume and N content in N-MCM-41-C are the reason for the low adsorption capacity for N-MCM-41-C. Even then, the adsorption capacity of N-MCM-41-C is much higher than the reported value (7×10^{-2} mmol.g^{-1}) for granule goetheite,[55] activated carbon[56] and Cu coordinated amino functionalized mesoporous silica.[57] Hence, N-MCM-41-E with a N content of 2.1 mmol.g^{-1} has superior adsorption capacity over many of the other reported adsorbents. N-MCM-41-E also showed higher adsorption capacity for Cr (VI) oxyanions, in comparison to N-MCM-41-D and N-MCM-41-C. However, the extent of uptake and saturation limit was found to be low for Cr (VI) oxyanion in comparison to As (V) oxyanion. This falling trend was noticed towards adsorption of As (V) or Cr (VI) ions. The removal

Table 2. Adsorptions of arsenate and chromate on amino-functionalized mesoporous silicas

Adsorbent	Concentration of $HAsO_4^{2-}$		K_d	Concentration of CrO_4^{2-}		K_d
	Initial (ppm)	final (ppm)		Initial (ppm)	final (ppm)	
N-MCM-41-D	1.5	0	$> 2.0 \times 10^6$	7.5	0	$> 2.0 \times 10^6$
	35	11.5	1.34×10^6	125	22.5	1.64×10^6
	210	23	1.78×10^6	255	28.5	1.77×10^6
N-MCM-41C	1.5	0	$> 2.0 \times 10^6$	7.5	0	$> 2.0 \times 10^6$
	33	7.5	1.53×10^6	125.5	17.5	1.72×10^6
	225	19.5	1.82×10^6	245	24.5	1.8×10^6
N-MCM-41-E	1.5	0	$> 2.0 \times 10^6$	7.5	0	$> 2.0 \times 10^6$
	37.5	13.5	1.28×10^6	125	16.5	1.73×10^6
	270	21	1.84×10^6	258	29	1.77×10^6

K_d = [anion adsorbed]/[anion in the solution]

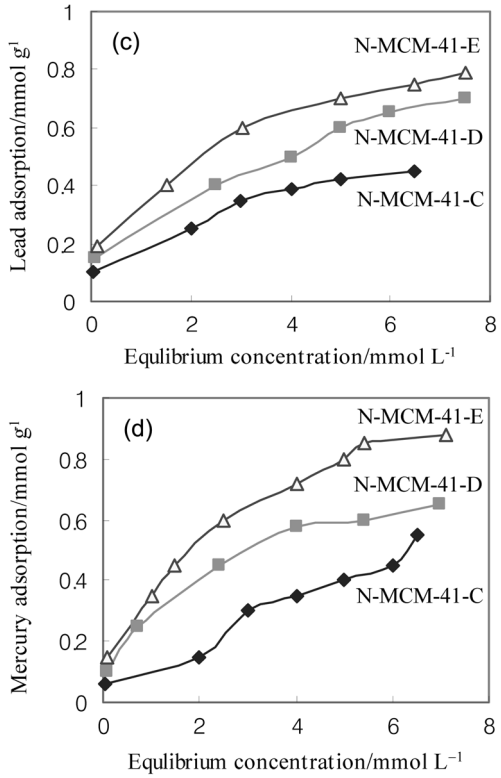

Figure 4. Adsorption isotherms of (c) lead and (d) mercury metal ions on functionalized MCM-41.

of Pb (II) and Hg (II) ions was followed using N-MCM-41-D, N-MCM-41-C and N-MCM-41-E (Fig. 4).

N-MCM-41-E showed higher adsorption for Pb (II) and Hg (II) ions in comparison to N-MCM-41-D and N-MCM-41-C (Table 3). The maximum adsorption for Pb (II) and Hg (II) by N-MCM-41-E was 0.78 $mmol.g^{-1}$ and 0.92 $mmol.g^{-1}$, respectively.

The adsorption of Hg (II) ions seems to the highest among the metal ions with N-MCM-41-E among three amine functionalized mesoporous materials. Undoubtedly, amine functionalized mesoporous silicas showed better efficiency for removal of metal ions from aqueous solutions. The order of removal of each metal ion by N-MCM-41-E is, Hg (II) < Pb (II) < As (V) < Cr (VI). The distribution coefficient (K_d) corresponding to the adsorption of metal ions, As (V), Cr (VI), Pb (II) and Hg (II) was calculated (Table 2 and 3) as the ratio of oxyanion adsorbed to oxyanion in solution. K_d was found to depend on the initial concentration of adsorbate ion. When the initial concentration of As (V), Cr (VI), Pb (II) and Hg (II) metal ions were ≤1.5 ppm, ≤7.5 ppm, ≤2.5 ppm and ≤4.0 ppm, respectively, there was no detectable metal ions in the solution after adsorption for 2 h (to the detection limit of ICP measurement). At these stages, the K_d values were $> 2 \times 10^6$, a higher value than noticed for mono, di and tri amino functionalized mesoporous silica prepared with dodecyltrimethyl ammonium chloride.[58] The variations in the extent of adsorption for Cr (VI), As (V), Pb

Table 3. Adsorptions of lead and mercury on amino-functionalized mesoporous silicas

Adsorbent	Concentration of Pb (II)		K_d	Concentration of Hg (II)		K_d
	Initial (ppm)	final (ppm)		Initial (ppm)	final (ppm)	
N-MCM-41-D	2.5	0	$> 2.0 \times 10^6$	4	0	$> 2.0 \times 10^6$
	47	17	1.27×10^6	56	21	1.25×10^6
	250	30	1.76×10^6	315	65	1.58×10^6
N-MCM-41C	2.5	0	$> 2.0 \times 10^6$	4	0	$> 2.0 \times 10^6$
	46	10	1.56×10^6	55	15	1.45×10^6
	255	36	1.71×10^6	300	46	1.69×10^6
N-MCM-41-E	2.5	0	$> 2.0 \times 10^6$	4	0	$> 2.0 \times 10^6$
	47	19	1.19×10^6	53	13	1.50×10^6
	295	31	1.78×10^6	330	34	1.79×10^6

K_d = [anion adsorbed]/ [anion in the solution]

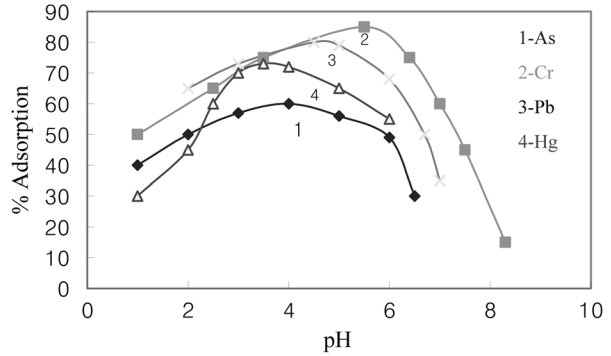

Figure 5. Effect of the pH on the percent adsorption of As (V), Cr (VI), Pb (II) and Hg (II) on N-MCM-41-E.

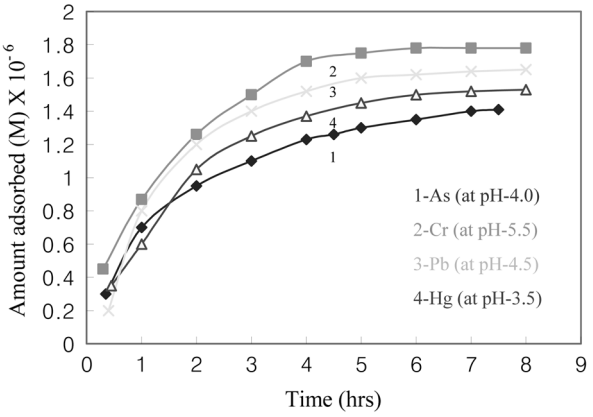

Figure 6. Effect of the contact times on adsorption of As (V), Cr (VI), Pb (II) and Hg (II) on N-MCM-41-E.

(II) and Hg (II) by N-MCM-41-D, N-MCM-41-C and N-MCM-41-E were followed in the pH range of 1.0-9.0 in (Fig. 5). Clearly, the extent of removal of metal ions, As (V), Cr (VI), Pb (II) and Hg (II), by N-MCM-41-D, N-MCM-41-C and N-MCM-41-E followed different pattern. The maximum removal of metal ions occurred at different pH ranges depending on the adsorbate-adsorbent pair.

For instance, N-MCM-41-E exhibited maximum adsorption for As (V), Cr (VI), Pb (II) and Hg (II) at 4.2, 6.2, 5.8 and 3.5 respectively. This behavior is attributed to arise from the existence of the metal ions in different forms in the pH ranges. For example, prominent Hg (II) species at lower pH (< 3.5) are predominantly as $Hg(NO_3)_2$ and $Hg(OH)NO_3$ or as $Hg(OH)_2$ at higher pHs (> 3.5). These species greatly affect the adsorption behavior of Hg (II) on the surface of adsorbent. The surface of amine functionalized MCM is expected to have affinity for negatively charged Hg (II) ions. The maximum adsorption for Hg (II) ions corresponds to the preferential removal of negatively charged Hg (II) by N-MCM-41-E (Fig. 5). At pHs higher than 3.5 Hg (II) may be changed into positively charged species and that may be the reason for the decrease in adsorption of Hg (II) by N-MCM-41-E beyond pH = 3.5. Similar explanation is applicable for explaining the adsorption behavior of other metal ions (Fig. 5).

After knowing the pH that was suitable to have higher metal ions removal for As (V), Cr (VI), Pb (II) and Hg (II), effect of time on the adsorption of these metal ions with N-MCM-41-E was followed. A concentration of 2×10^{-6} M was used to carry out the adsorption for metal ions. The experiments were carried out at the optimum pH of As (V), Cr (VI), Pb (II) and Hg (II) at 4.2, 6.2, 5.8 and 3.5 as determined from Figure 5. The results indicate the attainment of maximum adsorption within 5 h for all the heavy metal ions (Fig. 6).

Further, the metal ions were removed at a faster rate up to 2 h. Nearly 50% of the ultimate adsorption occurred within 2 h of contact time. Amine functionalized mesoporous materials prepared with surfactants having different length of alkyl chains show different adsorption capacities for few of the toxic metal ions. The extent of amine functionalization and relative decrease in textural parameters like pore diameter and pore volume are the influencing factors for the adsorption efficiency. These amine functionalized mesoporous materials are suitable for adsorption of toxic metal ions like arsenate, chromate, lead and mercury ions and show complete removal efficiency at lower concentration levels.

Conclusions

Amine functionalized mesoporous materials prepared with surfactants having different length of alkyl chains show different adsorption capacities for a few of the toxic metal ions. The extent of amine functionalization and relative decrease in textural parameters like pore diameter and pore volume are known to be the influencing factors for the adsorption efficiency. These amine functionalized mesoporous materials are suitable for adsorption of toxic metal ions like arsenate, chromate, lead and mercury ions and show complete removal efficiency at lower concentration levels.

Acknowledgment. This work was supported by Korea-China Joint Research Program (F01-2006-000-10119-0) and Korean Research Foundation (KRF 2006-J02402). The authors acknowledge Kyungpook National University Center for Scientific Instruments.

References

1. Kresge, C. T.; Leonowicz, M. E.; Roth, W. J.; Vartuli, J. C.; Beck, J. S. *Nature* **1992**, *359*, 710.
2. Beck, J. S.; Vartuli, J. C.; Roth, W. J.; Leonowicz, M. E.; Kresge, C. T.; Schmitt, K. D.; Chu, C. T.-W.; Olson, D. H.; Sheppard, E. W.; McCullen, S. B.; Higgins, J. B.; Schlenker, J. L. *J. Am. Chem. Soc.* **1992**, *114*, 10834.
3. Raman, N. K.; Anderson, M. T.; Brinker, C. J. *Chem. Mater.* **1996**, *8*, 1682.
4. Sayari, A.; Liu, P. *Micropor. Mesopor. Mater.* **1997**, *12*, 149.
5. Ciesla, U.; Schuth, F. *Micropor. Mesopor. Mater.* **1999**, *27*, 131.
6. Selvam, P.; Bhatia, S. K.; Sonwane, C. G. *Ind. Eng. Chem. Res.* **2001**, *40*, 3237.
7. Bae, J. Y.; Choi, S.-H.; Bae, B.-S. *Bull. Kor. Chem. Soc.* **2006**, *27*(10), 1562.
8. Cho, S.-Y.; Kim, N.-R.; Cao, G.; Kim, J.-G.; Chung, C.-M. *Bull. Kor. Chem. Soc.* **2006**, *27*(3), 403.

9. Barton, T. J.; Bull, L. M.; Klemperer, W. G.; Loy, D. A.; McEnaney, B.; Misono, M.; Monson, P. A.; Scherer, G. W.; Vartuli, J. C.; Yaghi, O. M. *Chem. Mater.* **1999**, *11*, 2633.
10. Huo, Q.; Margolese, D.; Stucky, G. D. *Chem. Mater.* **1996**, *8*, 1147.
11. Kruk, M.; Jaroniec, M.; Sakamoto, Y.; Terasaki, O.; Ryoo, R.; Ko, C. H. *J. Phys. Chem. B* **2000**, *104*, 292.
12. Lee, K.-P.; Showkat, A. M.; Gopalan, A.; Kim, S.-H.; Choi, S.-H. *Macromolecules* **2005**, *38*, 364.
13. Showkat, A. M.; Lee, K.-P.; Gopalan, A.; Kim, S.-H.; Choi, S.-H. *Polymer* **2005**, *46*, 1804.
14. Moller, K.; Bein, T. *Chem. Mater.* **1998**, *10*, 2950.
15. Brunel, D. *Micropor. Mesopor. Mater.* **1999**, *27*, 329.
16. Feng, X.; Fryxell, G. E.; Wang, L.-Q.; Kim, A. Y.; Liu, J.; Kemner, K. M. *Science* **1997**, *276*, 923.
17. Liu, J.; Feng, X.; Fryxell, G. E.; Wang, L.-Q.; Kim, A. Y.; Gong, M. *Adv. Mater.* **1998**, *10*, 161.
18. Kawi, S. *Chem. Commun.* **1998**, *13*, 1407.
19. Shen, S. C.; Kawi, S. *J. Phys. Chem. B* **1999**, *103*, 8870.
20. Liu, A. M.; Hidajat, K.; Kawi, S.; Zhao, D. Y. *Chem. Commun.* **2000**, *13*, 1145.
21. Brunel, D. *Micropor. Mesopor. Mater.* **1999**, *27*, 329.
22. Ehlers, L. J.; Pfeffe, M. J.; Melia, C. R. O. *Environ. Sci. Technol.* **2001**, *34*, 464.
23. Chen, S.-L.; Dzeng, S. R.; Yang, M.-H.; Chlu, K.-H.; Shleh, G. M.; Wal, C. M. *Environ. Sci. Technol.* **1994**, *28*, 877.
24. Nickson, R.; McArthur, J.; Burgess, W.; Ahmed, K. M.; Ravenscroft, P.; Rahman, M. *Nature* **1998**, *395*, 338.
25. Wittbrodt, P. R.; Palmer, C. D. *Environ. Sci. Technol.* **1995**, *29*, 255.
26. Sterrns, D. M.; Kennedy, L. J.; Courtney, K. D.; Giangrande, P. H.; Phieffer, L. S.; Wetterhahn, K. E. *Biochemistry* **1995**, *34*, 910.
27. Heary, L.; Ray, D. *Environ. Sci. Technol.* **1987**, *21*, 1187.
28. Baes, C. F.; Mesmer, Jr, R. E. *The Hydrolysis of Cations*; John Wiley and Sons: New York, U.S.A., 1976.
29. Roundhill, D. M.; Koch, H. F. *Chem. Soc. Rev.* **2002**, *31*, 60.
30. Harper, T. R.; Kingham, N. W. *Water Environ. Res.* **1992**, *64*, 200.
31. Fox, K. R.; Sorg, T. J. *J. Am. Water Works Assoc.* **1987**, *79*, 81.
32. De Carlo, E. H.; Thomas, D. M. *Environ. Sci. Technol.* **1985**, *19*, 538.
33. Min, J.; Eun, S. W.; Jae, K. P.; Sang, C. *Environ. Sci. Technol.* **2003**, *37*, 5062.
34. Toshiyuki, Y.; Takashi, T.; Hideaki, Y. *J. Colloid Interface Sci.* **2004**, *274*, 451.
35. Faust, S. D.; Ali, O. M. *Chemistry of Water Treatment*; Butterworth: Boston, U.S.A., 1983.
36. Mohan, D.; Guputa, V. K.; Srivastava, S. K.; Chander, S. *Colloids Surf. A* **2001**, *177*, 169.
37. Navarro, R. R.; Sumi, K.; Matumura, M. *Water Res.* **1999**, *33*, 2037.
38. Huang, C. P.; Hao, O. J. *J. Environ. Technol. Lett.* **1989**, *10*, 863.
39. Zamzow, M. J.; Eichbaum, B. R.; Sandgren, K. R.; Shanks, D. E. *Separ. Sci. Technol.* **1990**, *25*, 1555.
40. Mercier, L.; Pinnavaia, T. J. *Micropor. Mesopor. Mater.* **1998**, *20*, 101.
41. Celis, R.; Hermosin, M. C.; Cornejo, J. *Environ. Sci. Technol.* **2000**, *34*, 4593.
42. Feng, X.; Fryxell, E.; Wang, L.-Q.; Kim, Y.; Liu, J.; Kemner, K. M. *Science* **1997**, *276*, 923.
43. Mercier, L.; Pinnavaia, T. J. *Environ. Sci. Technol.* **1998**, *32*, 2749.
44. Liu, A. M.; Hidajat, K.; Kawi, S.; Zhao, D. Y. *Chem. Commun.* **2000**, 1145.
45. Zhang, L. Z.; Cheng, P.; Liao, D.-Z. *J. Chem. Phys.* **2002**, *117*, 5959.
46. Wei, Z.; Zhang, Z.; Wan, M. *Langmuir* **2002**, *18*, 917.
47. Ryoo, R.; Kim, J. K. *J. Chem. Soc. Chem. Commun.* **1995**, 711.
48. Ryoo, R.; Jun, S. *J. Phys. Chem. B* **1997**, *101*, 317.
49. Ryoo, R.; Ko, C. H.; Park, I. S. *Chem. Commun.* **1999**, 1413.
50. Mercier, L.; Pinnavaia, T. J. *Environ. Sci. Technol.* **1998**, *32*, 2749.
51. Zhao, X. S.; Lu, G. Q. *J. Phys. Chem. B* **1998**, *102*, 1556.
52. Autochshuk, V.; Jaroniec, M. *Chem. Mater.* **2000**, *12*, 2496.
53. Zhao, X. S.; Lu, G. Q.; Whittaker, A. J.; Millar, G. J.; Zhu, H. Y. *J. Phys. Chem. B* **1997**, *101*, 6525.
54. Diaz, J. F.; Balkus, K. J.; Bedioui, F.; Kurshev, V.; Kevan, L. *Chem. Mater.* **1997**, *9*, 61.
55. Hongshao, Z.; Stanforth, R. *Environ. Sci. Technol.* **2001**, *35*, 4753.
56. *Water. Polu. Conf. Fed.* **1978**, *50*, 993.
57. Fryxell, G. E.; Liu, J.; Hauser, T. A.; Nie, Z.; Ferris, K. F.; Mattigod, S.; Gong, M.; Hallen, R. T. *Chem. Mater.* **1999**, *11*, 2148.
58. Yoshitake, H.; Yokoi, T.; Tatsumi, T. *Chem. Mater.* **2002**, *14*, 4603.